The role of the exchange matrix in the itinerant-electron theory of ferromagnetism

1992 J. Phys.: Condens. Matter 4 L275

(http://iopscience.iop.org/0953-8984/4/16/005)

J. Phys.: Condens. Matter 4 (1992) L275–L280. Printed in the UK

LETTER TO THE EDITOR

The role of the exchange matrix in the itinerant-electron theory of ferromagnetism

J M Bass†, J A Blackman† and J F Cooke‡

† Department of Physics, University of Reading, Whiteknights, PO Box 220, Whiteknights, Reading RG6 2AF, UK

‡ Solid State Division, Oak Ridge National Laboratory, Oak Ridge, TN 37831, USA

Received 4 March 1992

Abstract. For HCP cobalt the spin-wave spectrum along the c-axis has been calculated, within the theory of itinerant-electron ferromagnetism, using the most general form of the electron–electron interaction exchange matrix. An attempt has been made to determine the relative magnitudes of the matrix elements, and the sensitivity of the spin-waves to the inclusion of the various distinct types of matrix elements is described.

Calculations based on the itinerant-electron theory of ferromagnetism have provided a good description of the low-temperature spin-wave spectrum of the cubic transition metals nickel and iron [1–3]. These calculations have predicted spin-waves above 100 meV in nickel and above 400 meV in iron. Subsequent experiments [4–6] have supported these results. One feature to have emerged from these calculations is the existence of multiple-spin-wave branches along the [001] direction. This follows quite naturally from a multi-band theory.

As a continuation of this work HCP cobalt is a natural candidate. As there are now two atoms in the unit cell, twice as many modes can be expected as in cubic systems, in addition to the extra structure from multi-band effects. A preliminary calculation on HCP cobalt has already been done [7]. This calculation used a highly simplified form of the electron–electron interaction exchange matrix. The calculations on nickel and iron, mentioned above, also used a very simple form of the exchange matrix. There has been previously an attempt [8], for the case of nickel, to include more general terms in the exchange matrix. A variety of behaviour in the spin-wave spectrum was observed. One general feature to emerge, however, was that the acoustic spin-wave close to the Γ-point was always well preserved.

In this letter the results of an attempt to determine the relative magnitudes of the matrix elements are reported with the aim of investigating how the various different terms affect the spin-waves. These matrix elements naturally group themselves into distinct types and thus the effect on the spin-wave spectrum can be examined by looking at the inclusion of these various types of matrix elements into the exchange matrix. The form factor was omitted from the previous calculation on HCP cobalt. In the calculations reported here the full form factor, which is dependent on the electronic wave functions, has been included.

0953-8984/92/160275+06$04.50

The theory on which this calculation is based is an extension of that described earlier [1–3] to two atoms per unit cell. The spin-polarized electronic wave functions are expanded in terms of tight-binding symmetry orbitals:

$$\psi_{nk\sigma}(r) = \sum_{l} \exp(ik \cdot l) \sum_{n\mu\sigma\lambda} a^{\lambda}_{n\mu\sigma} \phi^{\lambda}_{\mu}(r - l - \tau_{\lambda}) \exp(ik \cdot \tau_{\lambda}) \quad (1)$$

where n, k and σ are band, wave-vector, and spin labels, respectively. μ is a symmetry label which runs over the nine (s, p, d) symmetry terms and λ denotes the atom in the unit cell. l is a lattice vector and τ_{λ} is the position relative to a lattice site of atom λ in the unit cell. Within the random-phase approximation, the transverse part of the magnetic inelastic cross-section can be written as

$$\chi(Q, E) \simeq \sum_{\mu\nu\eta\xi\lambda\lambda'} F^{\lambda}_{\mu\nu}(Q)^* \left[\Gamma^{\lambda\lambda'}_{\mu\nu\eta\xi}(q, E)^{\text{ret}} - \Gamma^{\lambda\lambda'}_{\mu\nu\eta\xi}(q, E)^{\text{adv}} \right] F^{\lambda'}_{\xi\eta}(Q) \quad (2)$$

where F is the form factor given by

$$F_{\mu\nu}(Q) = \int \phi^*_{\mu}(r) \exp(iQ \cdot r) \phi_{\nu}(r) \, d^3r \quad (3)$$

and $Q = G + q$ with G a reciprocal-lattice vector and q restricted to the first Brillouin zone. The sum in (2) is taken over only the d-symmetry terms which are the dominant ones. Γ is the enhanced Green's function defined by

$$\Gamma(q, z) = [I + G(q, z)W]^{-1} G(q, z) \quad (4)$$

and the unenhanced Green's function G is given by

$$G^{\lambda\lambda'}_{\mu\nu\eta\xi}(q, z) = N^{-1} \sum_{nmk} \frac{a^{\lambda}_{n\mu\downarrow}(k)^* a^{\lambda}_{m\nu\uparrow}(k+q) a^{\lambda'}_{n\eta\downarrow}(k) a^{\lambda'}_{m\xi\uparrow}(k+q)^*}{z - E(m, k+q, \uparrow) + E(n, k, \downarrow)} \times (f_{nk\downarrow} - f_{mk+q\uparrow}). \quad (5)$$

Note that the wave-function expansion coefficients are generally complex, which is why it is necessary to consider the retarded and advanced Green's functions specifically in (2). $f_{nk\sigma}$ are the Fermi occupation numbers and $W^{\lambda\lambda'}_{\mu\nu\eta\xi}$ are matrix elements of a self-consistently screened electron–electron interaction:

$$W^{\lambda\lambda'}_{\mu\nu\eta\xi} = \int \phi^{\lambda}_{\mu}(r) \phi^{\lambda'}_{\nu}(r') U_{\text{sc}}(r, r') \phi^{\lambda'}_{\eta}(r') \phi^{\lambda}_{\xi}(r) \, d^3r \, d^3r'. \quad (6)$$

Within the RPA the electronic energy is written as

$$E(n, k, \sigma) = \epsilon(n, k, \sigma) + \sum_{\mu\nu\eta\lambda\lambda'} a^{\lambda}_{n\mu\sigma}(k)^* a^{\lambda}_{n\nu\sigma}(k) W^{\lambda\lambda'}_{\mu\nu\eta\eta} \left(N^{\lambda\uparrow}_{\eta} - N^{\lambda'\downarrow}_{\eta} \right) \quad (7)$$

where $\epsilon(n, k, \sigma)$ is the energy in the absence of the electron–electron interaction, and $N^{\lambda\sigma}_{\mu}$ is the number of electrons of symmetry type μ on site λ in the unit cell and with spin σ:

$$N^{\lambda\sigma}_{\mu} = N^{-1} \sum_{nk} |a^{\lambda}_{n\mu\sigma}(k)|^2 f_{nk\sigma}. \quad (8)$$

The band-structure input of the calculation comes from an empirical Slater–Koster parametrization [9], adapted to hexagonal systems by Miasek [10]. Papaconstantopoulos [11] has given orthogonal two-centre parameters for paramagnetic bands, which were obtained by fitting to a first-principles augmented-plane-wave calculation. For these calculations zero temperature was assumed. This approximation was not considered likely to present problems as, for cobalt, the Curie temperature is $\simeq$ 1400 K, so the results should also be valid at room temperature. Furthermore, as these calculations require large amounts of computer time, it has only been possible, so far, to calculate the spin-wave dispersion along the c-axis in the Γ–A direction where significant economy in computation is possible because of symmetry.

The previous calculations on HCP cobalt took the matrix elements in the exchange matrix (6) to be purely diagonal; that is, only the terms $W^{\lambda\lambda}_{\mu\mu\mu\mu}$ were taken to be non-zero and as, a further simplification, all of these diagonal terms were set equal. This gave a single parameter which determined both the band splitting through (7) and the enhancement to the Green's functions. A value of this parameter, of 0.37 Ryd, was obtained by fitting the calculated magnetization to the experimental value of 1.6 μ_B/atom. The justification for retaining only the diagonal terms of the exchange matrix was based on the belief that these terms would be dominant. Actually the assumption of a purely diagonal exchange matrix violates certain symmetry requirements. This is because, as there are symmetry operations connecting the different d-orbitals, there are therefore relations connecting the different terms in the exchange matrix. For the HCP structure there are, in fact, fourteen distinct matrix elements which can, for the sake of this analysis, be divided into four types by virtue of the pairing of their indices. These are listed and labelled in table 1. In addition to the matrix elements listed in the table there are two terms W_{1441} and W_{2332}, nominally of type B, which can be given in terms of terms of types A and C through the relations $W_{1111} = W_{1441} + 2W_{1144}$ and $W_{2222} = W_{2332} + 2W_{2233}$. It is therefore not permissible to include terms of type A without also including the terms W_{1144} and W_{2233}, or W_{1441} and W_{2332}, or both. That is to say that if the magnitudes of W_{1111} (W_{2222}) and W_{1144} (W_{2233}) are fixed then it is necessary also to include a term W_{1441} (W_{2332}).

Table 1. The four types of the fourteen distinct matrix elements of the electron–electron interaction exchange matrix. The indices 1,2,3,4 and 5 refer to the z-components of the angular momentum, of the d-orbitals, with quantum numbers −2, −1, 1, 2 and 0 respectively.

Type	Matrix elements
A	W_{1111} W_{2222} W_{5555}
B	W_{1221} W_{1551} W_{2552}
C	W_{1122} W_{1155} W_{2255} W_{1144} W_{2233}
D	W_{1243} W_{1235} W_{1253}

In order to get a better feel for the relative size of the matrix elements a simple calculation was performed in which an unscreened Coulomb potential was taken in (6). This could then be expanded into a radial part and a sum of spherical harmonics. The wave functions could likewise be expanded reducing the problem to an angular part, given by a sum of Gaunt coefficients, and a radial integral which could be solved analytically with a suitably chosen form for the radial wave function. It was

found that the diagonal terms were indeed the largest and those of type B were of a similar magnitude, whereas those of type C were smaller by a factor of twenty and those of type D were smaller by a factor of forty. To get a fix on the absolute size of these matrix elements they could then be adjusted, whilst retaining their relative magnitudes, to give the experimental value of the magnetization. Note that only terms of type A and C feature in (7), which is the expression linking the elements of the exchange matrix with the magnetization. Although an unscreened Coulomb potential was used in this simple calculation it is believed that the ratio of the various terms would not change much if a screened Coulomb potential were to be used.

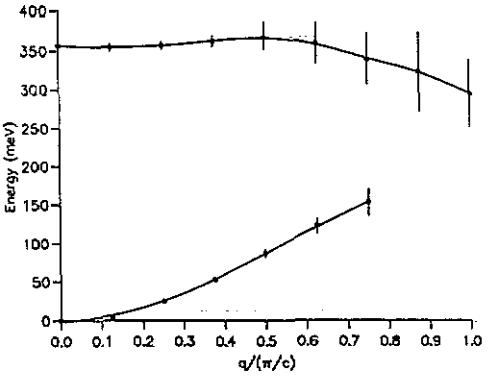

Figure 1. Spin-wave dispersion for q (in units of π/c) along the Γ–A direction for an electron–electron interaction exchange matrix containing terms of types A and C. Vertical lines show the width (FWHM) of the inelastic neutron scattering peaks.

In figure 1 the spin-wave dispersion along the Γ–A direction is plotted, for an exchange matrix containing the full set of terms of types A and C together with the terms W_{1441} and W_{2332} necessary to ensure that the symmetry condition is satisfied. The terms of type C were taken to be 0.05 times the size of those of type A, so W_{1441} and W_{2332} had to be taken to be 0.9 times the size of the terms of type A. From figure 1 it can be seen that there is an acoustic branch which extends nearly all the way to the zone boundary and an optic branch existing all the way to the zone boundary. The acoustic branch has been drawn only for q-values up to $0.75\pi/c$. At the next value of q for which calculations were made ($0.875\pi/c$), the acoustic branch appears as a shoulder in the, by now, more intense optic branch and is not resolved as a separate peak. Referring to the acoustic branch the spin-wave stiffness was calculated to be 610 meV Å^2. This compares to a value of 560 meV Å^2 at 0 K determined experimentally [12] in low-energy neutron measurements up to about 25 meV. In figure 2 the spin-wave dispersion for an exchange matrix containing terms of types A and B, together with the terms W_{1441} and W_{2332}, is plotted. For this case the terms of type B and W_{1441} and W_{2332} were taken to be the same size as the terms of type A, so it was not necessary to include any terms of type C. Here there is a much richer structure than in the case above, with four distinct spin-wave branches, none of which are present along the entire length of the symmetry direction. Notice also that these spin-waves are very much lower in energy than those in figure 1. The distinction between the spin-waves drawn with full lines and those drawn with dashed lines will be explained below. For this choice of exchange matrix the spin-wave stiffness were calculated to be 320 meV Å^2. Three more forms of exchange matrix were investigated. The first of these contained terms of types A, B and C, the second contained terms of all four types and the third contained all four types of

term with each of the fourteen distinct matrix elements adjusted to make their relative magnitudes the same as those obtained from the simple calculation outlined above. All three of these exchange matrices necessarily contained the additional two terms W_{1441} and W_{2332}. The spin-wave dispersion was found to be nearly identical for all three cases. The results for the latter of these three forms are shown in figure 3. Here there is a similar picture to figure 1 but with the optic branch being lower in energy. However, unlike in figure 3, the acoustic branch ends abruptly just after the last plotted point at 3/4 of the distance to the zone boundary. With all three of these forms of exchange matrix the spin-wave stiffness was calculated to be 350 meV Å^2.

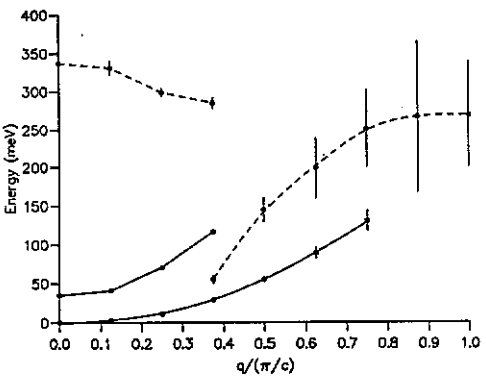

Figure 2. As figure 1, but for an exchange matrix containing terms of types A and B.

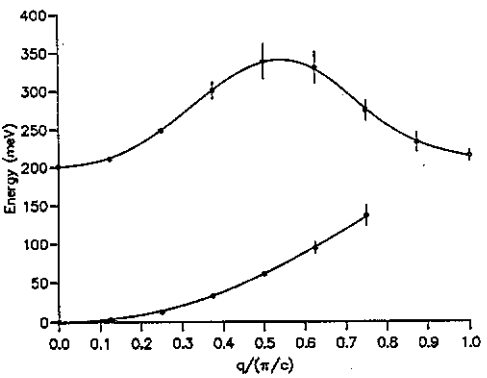

Figure 3. As figure 1, but for the most general form of exchange matrix.

In local-moment theories it is expected that the relative intensities of the acoustic and optic spin-wave branches should depend on the reciprocal-lattice vector G around which the scattering is observed. For example, scattering around $G = (0,0,0)$ will give the scattering weight entirely in the acoustic branch, whereas scattering around $G = (0,0,2\pi/c)$ will give the scattering weight entirely in the optic branch and scattering around $G = (2\pi/a, 2\pi/a\sqrt{3}, 0)$ will give a scattering weight distributed between both branches. For the itinerant model at the Γ point this is indeed the case, but as the electrons are now considered to have band behaviour, then away from this point the effect of the form factor now becomes important.

For the Γ point it was found that for scattering around $G = (0,0,\pm 2n\pi/c)$ with n even, all the scattering weight was in the acoustic branch as expected. However, as one moves away from the Γ point in the Γ–A direction, then the scattering weight gradually shifts from the acoustic branch to the optic branch. For scattering around $G = (0,0,\pm 2n\pi/c)$ with n odd, the opposite is observed. There is a shift in the scattering weight from the optic branch to the acoustic branch. In figure 2 where there are four branches to the spin-wave spectrum, those drawn with full lines have maximum intensity for scattering around $G = (0,0,\pm 2n\pi/c)$ with n even, and those drawn with dashed lines have maximum intensity for scattering around $G = (o,0,\pm 2n\pi/c)$ with n odd. A more detailed account of the effects of including the form factor will be published elsewhere.

Finally, these results show that the inclusion of the various different terms into the electron–electron interaction exchange matrix can produce a variety of spin-wave behaviour. In particular the optic spin-wave was very sensitive to the exact form of the exchange matrix. It was found that terms of the form $W^{\lambda\lambda}_{\mu\mu\nu\nu}$, even though very small, were critical in fixing its exact position. Experimental data will now be very important in pinning down the details of the model. The general picture that seems to be emerging both here and in the earlier work [7], which only included the diagonal elements of the exchange matrix, is that of an acoustic branch of well defined spin-waves reaching an energy of $\simeq$ 150 meV at about 3/4 of the way to the zone boundary. Work is currently under way to evaluate the elements in the exchange matrix, using a screened Coulomb potential, with the screening length taken as the single variable parameter. This, together with better neutron scattering data, will provide the most rigorous test yet of the itinerant-electron theory of ferromagnetism.

We wish to thank Dr G-Y Guo of the Daresbury Laboratory for providing us with a potential for HCP cobalt. This research was funded in part by the Science and Engineering Council and in part by the Division of Material Sciences, US Department of Energy under Contract No DE-AC05-840R21400 with Martin Marietta Energy Systems, Inc.

References

[1] Cooke J F, Lynn J W and Davis H L 1980 *Phys. Rev.* B **21** 4118
[2] Cooke J F, Blackman J A and Morgan T 1985 *Phys. Rev. Lett.* **54** 718
[3] Blackman J A, Morgan T and Cooke J F 1985 *Phys. Rev. Lett.* **55** 2814
[4] Mook H A and DMcK Paul 1985 *Phys. Rev. Lett.* **54** 227
[5] DMcK Paul, Mitchell P W, Mook H A and Steigenberger U 1988 *Phys. Rev.* B **38** 580
[6] Perring T G, Boothroyd A T, DMcK Paul, Taylor A D, Osborn R, Newport R J, Blackman J A and Mook H A 1991 *J. Appl. Phys.* **69** 6219
[7] Trohidou K N, Blackman J A and Cooke J F 1991 *Phys. Rev. Lett.* **67** 2561
[8] Cooke J F and Blackman J A 1988 *J. Physique Coll.* **49** C8 81
[9] Slater J C and Koster G F 1954 *Phys. Rev.* **94** 1498
[10] Miasek M 1957 *Phys. Rev.* **107** 92
[11] Papaconstantopoulos D A 1986 *Handbook of the Band Structure of the Elemental Solids* (New York: Plenum)
[12] Shirane G, Minkiewicz V J and Nathans R 1968 *J. Appl. Phys.* **39** 383